Overview of TJ-II experiments

J. Sánchez, M. Acedo, D. Alegre, A. Alonso, J. Alonso, P. Álvarez, J. Arévalo, E. Ascasíbar, A. Baciero, D. Baião1), L. Barrera, E. Blanco, J. Botija, A. Bustos, E. de la Cal, I. Calvo, A. Cappa, D. Carralero, R. Carrasco, B.A. Carreras2), F. Castejón, R. Castro, G. Catalán, A.A. Chmyga3), M. Chamorro, L. Eliseev4), L. Esteban, T. Estrada, J.A. Ferreira, J.M. Fontdecaba, L. García5), R. García-Gómez, J.M. García-Regaña, P. García-Sánchez, A. Gómez-Iglesias, S. González, J. Guasp, T. Happel, J. Hernanz, J. Herranz, C. Hidalgo, J.A. Jiménez, A. Jiménez-Denche, R. Jiménez-Gómez, I. Kirpitchev, A.D. Komarov3), A.S. Kozachok3), L. Krupnik3), F. Lapayese, M. Liniers, D. López-Bruna, A. López-Fraguas, J. López-Rázola, T. Madeira1, F. Martín-Díaz, F. Martín-Hernández, A.B. Martín-Rojo, J. Martínez-Fernández, K.J. McCarthy, F. Medina, M. Medrano, L. Melón, A.V. Melnikov4), P. Méndez, B. van Milligen, E. Mirones, A. Molinero6) , M. Navarro, I.S. Nedzelskiy1), M. Ochando, J. Olivares, E. Oyarzábal, J.L. de Pablos, L. Pacios, I. Pastor, M.A. Pedrosa, A. de la Peña, A. Pereira, A. Petrov4), S. Petrov7), A. Portas, G. Rattá, J.M. Reynolds8), E. Rincón, L. Ríos, C. Rodríguez, B. Rojo, J.A. Romero, A. Ros, M. Sánchez, E. Sánchez, G. Sánchez-Burillo, E. Sánchez-Sarabia, K. Sarksian9), J.A. Sebastián, C. Silva1), E.R. Solano, A. Soleto, F. Tabarés, D. Tafalla, J. Tera, A. Tolkachev, J. Vega, G. Velasco, J.L. Velasco, M. Weber, G. Wolfers and B. Zurro

Laboratorio Nacional de Fusión, Asociación EURATOM/CIEMAT, 28040, Madrid, Spain.
1) Associação EURATOM/IST, Instituto de Plasmas e Fusão Nuclear. Av. Rovisco Pais, 1049-001 Lisboa. Portugal
2) BACV Solutions Inc., Oak Ridge, TN 37830, USA
3) Institute of Plasma Physics, NSC KIPT, 310108 Kharkov, Ukraine
4) Institute of Nuclear Fusion, RNC Kurchatov Institute, Moscow, Russia
5) Universidad Carlos III, Madrid, Spain
6) Laboratorio General de Electrónica y Automática – CIEMAT, Miguel Navarro Santana
7) A.F. Ioffe Physical Technical Institute, 26 Polytekhnicheskaya, St Petersburg, Russia
8) BIFI, Universidad de Zaragoza, 50009-Zaragoza, Spain
9) General Physics Institute, Russian Academy of Sciences, Moscow, Russia

E-mail contact of main author: joaquin.sanchez@ciemat.es

Abstract. This paper presents an overview of experimental results and progress made in investigating particle control using Li-coating, transport and L-H transitions in TJ-II. The Li coating changes drastically the plasma-wall interaction, decreasing the recycling, and enlarges substantially the operational range of the device avoiding the appearance of radiative collapse, which permits to study confinement properties at much higher densities. Moreover, L-H mode transition has been only achieved after Li-coating in TJ-II. The effect of rationals on heat transport is studied showing a decrease of heat diffusivity close to their position, and it is also seen that rationals located in the edge make L-H transition easier. TJ-II findings provide a new guideline for understanding the trigger mechanism of the L-H transition pointing out the importance of low frequency fluctuating sheared ExB flows. The properties of fast ion confinement are also described as well as the effects of impurities on radiation profiles, showing two types of profiles the "bell" and the "dome" shape, being the latter more robust under radiative collapse.

1. Introduction.

Global confinement and accessibility to improved confinement regimes is strongly linked to the magnetic topology in fusion plasmas. The flexibility of stellarator devices makes them ideal laboratories to study the relation between magnetic topology, electric fields and transport. In particular, the specific characteristics of the stellarator TJ-II, *i.e.* low magnetic

shear and high magnetic configuration flexibility in the iota profile, allow controlling the position of low order rational values within the rotational transform profile and, therefore, the study of how the magnetic topology affects on transport and global confinement. An effort is also done in stellarator optimization in order to find a stellarator configuration check the possibility of finding an optimised stellarator with the same flexibility properties as TJ-II [1].

Recent improvements in plasma diagnostics have led to a better understanding of the confinement properties of TJ-II, including a two-channel Doppler reflectometer for electric field studies [2], Heavy Ion Beam Probe diagnostic for the characterization of plasma potential, plasma density and their fluctuations [3], diagnostics for long-range correlation studies making use of two fast reciprocating Langmuir probes arrays located at two different toroidal positions [4], supersonic He beam for ion temperature measurements [5], suprathermal ion detection by spectroscopy and luminescent probe [6], the development of a dedicated neutral beam injection system and charge-exchange diagnostic [7], two-colour infrared interferometer [8], implementation of multi-filter photodiodes for core electron temperatures [9] and advanced data processing techniques [10].

The results presented in this paper were obtained in plasmas created and heated by Electron Cyclotron Resonance Heating (ECRH) (2 x 300 kW gyrotrons, at 53.2 GHz, 2^{nd} harmonic, X-mode polarisation) and Neutral Beam Injection (NBI). The ECRH was coupled to the plasma via two quasi-optical transmission lines, placed at stellarator-symmetric positions, equipped with an internal steerable mirror. Beams of 400 kW port-through (H_0) power at 30 kV, were injected into target plasmas created using one or both gyrtrons. Ongoing TJ-II experiments are focussed on studying the efficiency of Electron Bernstein Waves (EBW) heating system using the OXB mode conversion scenario. Previous studies [11] predict efficient plasma heating by EBW that must be checked experimentally. Those waves are also very efficient to drive non-inductive currents due to the fact that resonate with fast low-collisional electrons, and hence can modify the rotational transform profile and compensate the bootstrap current [12], with the limitation of the small control one has on the power deposition profile. The estimates of the bootstrap current, which is very challenging for the complex TJ-II geometry, has been performed together with the EBCD [13].

The paper is organised as follows: In section 2, the role of Li-coating on TJ-II particle control is discussed. Confinement and configurations effects are discussed in section 3. L-H transition in TJ-II is discussed in section 4. Finally, conclusions are presented in section 5.

2. Li-coating experiments and particle control by gas injection.

Great improvement of plasma particle control has been observed in the TJ-II stellarator after Li-coating [14], in comparison with the operation under Boron coated walls. The beneficial Li properties for plasma-wall interaction have a strong effect on this device that presents a helical limiter very close to the magnetic axis, which receives the strongest particle and heat fluxes. In boron-coated wall plasmas a systematic, steady density ramp up was observed as the beam power was switched on. This fast density build-up, being limited the available heating power, led, generally, to a relatively quick plasma termination due to radiative collapse, for line density values below $3 \times 10^{19} m^{-3}$. Under lithium conditions this lack of density control has been dramatically improved and long, stationary density plateaus (up to ten energy confinement times) can be achieved, allowing density scans with the help of external gas puff, as shown in Figure 1 [15]. It illustrates the difference between both wall scenarios as regards the behaviour of energy content and confinement time, for NBI

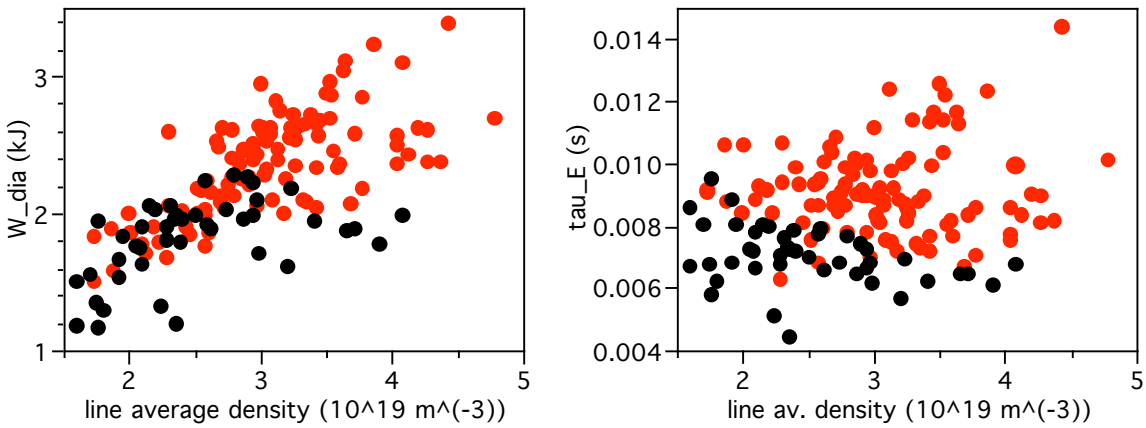

***Figure 1**: Maximum value of the plasma energy content (left) and energy confinement time (right) vs.plasma density for B-coated (black) and Li-coated walls (red symbols).*

discharges using the co-injector with comparable heating power and the same magnetic configuration [16]. In order to get some insight into the underlying physics, a systematic comparison of the global particle and energy balance under both wall scenarios and otherwise identical main plasma parameters has been recently addressed. It was concluded that for the overlapping parametric space, and in particular for ECR Heated plasmas, no major difference in the 0-dimensional analysis can be seen.

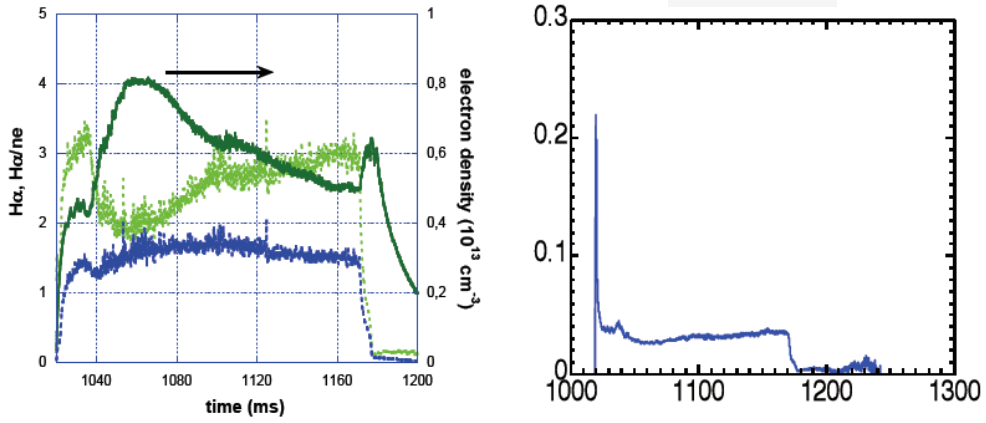

***Figure 2**. Left: time traces of Ha (lower trace), electron density (right) and ratio between them (upper trace, left) for a He, ECRH plasma on a hydrogenated Li wall. Right: Deduced hydrogen desorption yield for He on Li:H for the same discharge.*

In the last campaigns, an important effort has been devoted to the understanding of the sputtering and retention characteristics of the Li layers, and their possible interconnection [17]. The very low value of H recycling under the film coating technique used in TJ-II (Li on top of a B layer), R ~ 0.1, warrants density control in gas puffed or NBI fuelled plasmas, as it has been described elsewhere [14]. For He, values as low as R~ 0.82 have been deduced from steady state or perturbative puffing experiments at room temperature. Recently, desorption of H trapped into the Li film by the He plasma discharge has been addressed. Of particular interest is to check whether a He plasma ejects both species from the film (H and Li) with similar or distinct energy threshold and yields. In the first case, the sputtering of some short of molecular entity (such as LiH for example) would be expected, the resulting individual emissions being produced by plasma fragmentation. On the contrary, although similar absolute values for the corresponding yields are predicted by the TRIM code for a

pure Li layer [17], different energy dependence should be observed, as expected from different threshold values. However, the fact that strong material mixing is expected upon plasma exposure of the coating, leading to surface dilution and chemical bonding effects, makes it very difficult to assess how the ratio of H to Li ejection should behave in reality. Furthermore, the ratio of neutral to ionic sputtering yields, assumed to be 1/3 for metallic lithium could be strongly modified by the presence of more electronegative species (C, B) in the mixture. In Figure 2, the release of H by He plasma (b) and the line average density together with the density normalized H_α emission (a) are depicted. A fairly constant yield, of γ~0.03-0.04 is deduced for this particular discharge. The analysis of other similar discharges yields value between 0.02 and 0.06, in very good agreement with TRIM code estimates and making allowance for the intrinsic uncertainties in the estimates.

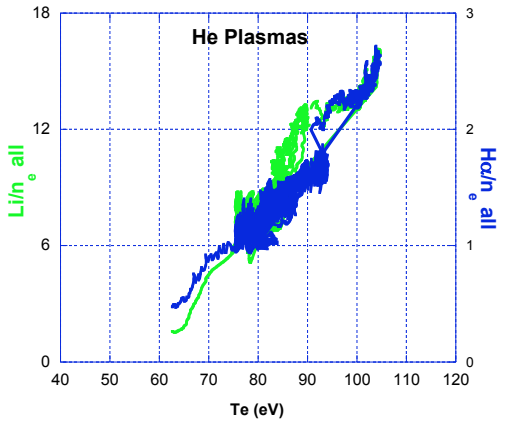

***Figure 3**. Dependence of the Li emission and Ha signal, both density -normalized, with the LCFS electron temperature*

Figure 3 shows the dependence of the Li emission and the H_α signal, both density-normalized, with the electron temperature [17]. Two important facts are worth highlighting in the data shown in the figure. First, a very similar threshold energy, corresponding to electron temperatures of T_e ~ 50 eV, seems to exist for both processes, obviously higher than the expected ones from TRIM calculations (E_{th} ~ 9 eV for Li sputtering by He^+). Secondly, the same energy dependence seems to apply for H desorption and Li sputtering, two distinct processes in terms of standard sputtering theory.

Finally, the release of glow discharge implanted He by a H plasma, followed by emission of He (at 667 nm) in the plasma and by mass spectrometry, normalized to the particle flux was followed in a shot by shot basis [17]. Fitting of the decay of He during the first shots yields a characteristic time constant of ~ 0.5 s, corresponding to a total ion flux of 0.5 x 10^{17} cm^{-2}, and hence a cross section, s, of ~2 x 10^{-17} cm^{-2} can be deduced assuming first order desorption kinetics. This value is to be compared to the cross sections obtained for the reverse process, i.e. desorption of H in He plasma. A value of σ =4 x $10^{-17}cm^2$ was deduced from glow discharge (GD) laboratory plasmas on pure Li coatings, while a factor of 6 higher value was obtained in GD conditioning of TJ-II, possibly associated to the contribution from the B/C coating to the H retention characteristics of the film. As seen in the figure, a steady value of He desorption is reached after a few shots. This behaviour was also apparent during GD conditioning of a He saturated Li wall by a H plasma and it is interpreted as a diffusion-limited release process, thus implying that refilling of the topmost layer, which is He-depleted by H bombardment in every shot, takes place between shots. Experiments with different time delay between shots are now in progress in order to characterize the corresponding diffusion coefficient.

A key ingredient for understanding the operational improvement is the profile radiation under Li coated wall. Edge radiation can be kept small avoiding the power unbalance that triggers the low radiation collapse. These profiles (with strong pressure gradients and enhanced central confinement, concomitant to central impurity accumulation) are observed to spontaneously transit to broader profiles (with lower-central Z_{eff} values) when

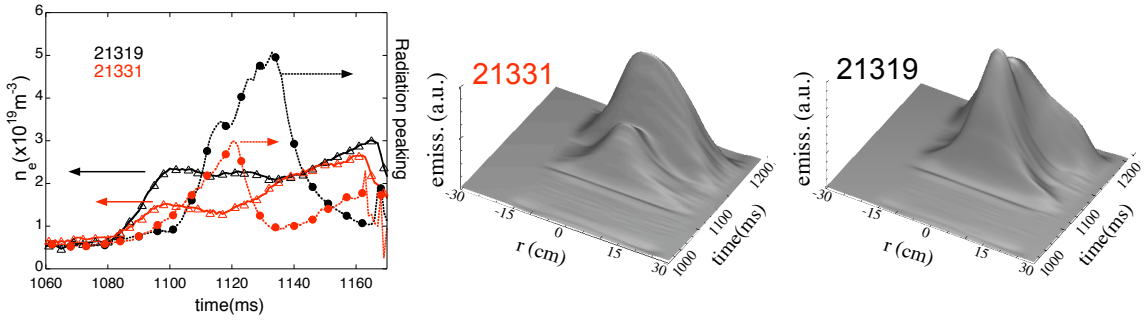

***Figure 4**. a) Radiation peaking and b) radial profiles evolution for spontaneous (#21319) and forced (#21331) transitions.*

approaching the density limit. Profile shapes have been tagged as "bell" and "dome" type, respectively, and the transition between them during a shot, is regularly classified and followed from bolometric data. Perturbative experiments (using H_2, mixtures of H_2+ Ne, and N_2 gas injection) were performed to force the bell-to-dome profile transition at moderate densities, far from the "spontaneous" transition conditions (see Fig. 4 a) and b). The detailed dynamics of profile change consisted in an almost simultaneous edge increase and core decrease of radiation, and it was essentially the same under diluted Ne or H_2 injections. This response was found compatible with enhanced peripheral charge-exchange processes that diminish the coupling of fast neutrals with the plasma core (i.e., reduces density peaking), and may favour the development of thermal instability-driven plasma collapse. With the aim of trying to find a method to control the density rise through the reduction of wall sputtering via edge radiation cooling, during the last experimental campaign, other non-intrinsic low-Z

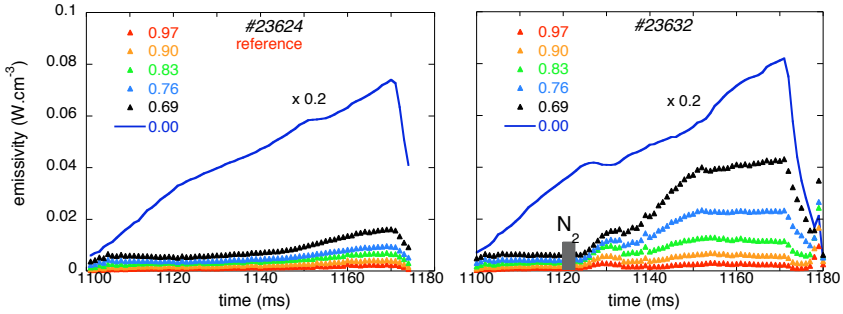

***Figure 5.** Time evolution of plasma emissivity at the indicated effective radii. The 4 ms length N_2 pulse starts at 1120 ms in shot # 23632.*

impurity species, namely N_2, has been injected. What was observed is that adequate amounts of this impurity may establish a quasi-stationary radiation enhanced region at the plasma periphery (see Fig. 5).

By comparing discharges with injection and their reference shots in different magnetic configurations, what we found is that the deepest radial location in which we see the maximum positive perturbation in radiation due to impurity entrance varies, and coincides with the nominal location of significant rational surfaces [18].

Laser blow-off has been used to inject trace boron impurities to study impurity transport. The parallel transport of boron ions has been measured with two filter-copes monitoring B-II

line on opposite sides of the torus. Following the initial fast parallel propagation of boron ions, a slower (above 10 ms) global confinement of impurities has been investigated in ECRH and NBI plasmas. Boron confinement times are similar to those previously observed for Fe [19].

The injection of impurities can be followed with the multi-filter soft X-ray diagnostic, where the calculated T_{e0} shows the rapid cooling due to the impurity entrance. Moreover, with the help of the impurity transport code IONEQ, it is possible to simulate the expected soft X-ray emissivities assuming particular plasma contaminants. These simulations provide extra information about the evolution of impurities present in the plasma and how they influence the electron temperature, which can be cross-checked with other TJ-II diagnostic systems.

3. Confinement and configuration effects.

Confinement studies in ECH plasmas show reduced values for the effective electron heat diffusivity in regions where the lowest order magnetic resonances are located [20]. The result is especially interesting after considering the low magnetic shear configurations of this device. The measurements [21] clearly indicate changes in the electric field related with the location of magnetic resonances; in addition, kinetic calculations [22] based on collisional transport alone show 3D plasma current densities able to modify the magnetic structure in the resonant regions, even in the absence of electric fields [20]. Both elements, radial electric field and plasma currents in the resonant regions, are also important in other phenomena like the formation of internal electron-heat barriers or the healing of islands in helical devices [23]. Tracking effects of magnetic resonances in the electron heat effective diffusivity has also been investigated.

A transition from kinetic effect-dominated to a more collisional regime is found in ECRH plasmas. The electric field, positive all over the plasma in the low ECRH plasma regime, starts developing negative values at the maximum density gradient region when the collisionality reaches a threshold value. Further increments in the density extend the region with negative electric fields towards the plasma centre. In the lithium-coated NBI plasmas studied in this paper, plasma density has been varied in the range $1.7\times10^{19} m^{-3} \le \bar{n}_e \le 6.1\times10^{19} m^{-3}$, the energy confinement time, t_E, ranging from 3 to 14 ms. Regression analysis of τ_E indicates stronger degradation with heating power (power exponent – 0.8) and similar density dependence (power exponent 0.5) as compared to ISS04 [16].

During the NBI heating phase broad spectral structures that straddle intense emission lines from multiply ionized oxygen lines are observed by a normal-incidence spectrometer viewing a plasma region well separated from the neutral beam/ plasma interaction volume [24]. It has been demonstrated that their source is fast oxygen ions that originate as accelerated H_2O and H_3O ions in the ion sources of the NBI. Once neutralized in the neutralization chamber they penetrate the plasma where they are reionized, confined and perform multiple toroidal transits of the TJ-II before being lost or slowed down. On the one hand these findings have implications for the analysis of oxygen spectral lines during NBI heating phases in TJ-II, and possibly other magnetically confined plasma devices. On the other hand such emissions may provide a tool for studying phenomena such as fast-ion slow down and confinement, or the influence of NBI injection direction and BT on fast ions as the observations demonstrate the possibility of employing neutral beams doped with a suitable impurity element, if not already doped with oxygen, in combination with strategically

positioned spectroscopic instruments, to probe such behaviour in hot magnetically confined plasmas.

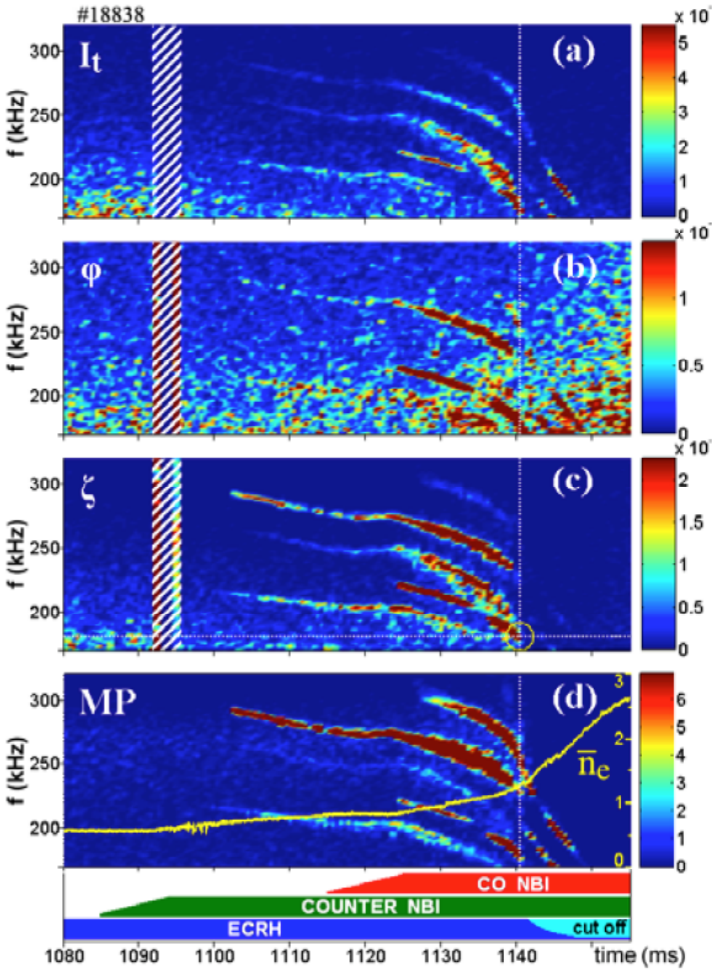

Figure 6. *Power spectra time evolution of HIBP (ρ = 0.5) and Mirnov probe signals. Alfvén Eigenmodes are clearly observed in (a) the total HIBP secondary beam current; (b) on the potential;(c) on the toroidal shift of secondary beam ζ proportional to Bpol;(d) on the Mirnov probe signal. The line-averaged density is also shown in (d). Instrumental gaps in HIBP signal are shown by hatched ribbons in (a, b, c).*

Alfven eigenmodes (AEs) destabilized in NBI plasmas [25], also related to low order resonances, can influence fast ion confinement. The dynamics of fast ions coming from NBI is also estimated for TJ-II using the code ISDEP, which allows one to estimate the slowing down time, the confinement and distribution function of these ions in order to compare these results with the CX-NPA measurements [26].

Recently the Heavy ion beam probing (HIBP) system has become a new tool to study AEs with high spatial and frequency resolution [3]. AEs are pronounced in the local density, electric potential and poloidal magnetic field oscillations, detected simultaneously by HIBP in the frequency range 50 kHz < f_{AE} < 300 kHz. Various AE modes are visible in the neutral beam injector (NBI)-heated plasma for co-NBI (400 kW), counter- (400 kW) and balanced NBI (800 kW) from the plasma centre to the edge. A high coherence between magnetic probes and HIBP data was found for specific AEs. When the density rises, AE frequency decreases and the cross-phase between the plasma density, poloidal magnetic field and potential remains constant. The amplitude of the AE potential oscillations are in the order of 10 V with poloidal electric fields in the order of 10 V /cm. AEs may bring small or significant contribution to the turbulent ExB particle flux depending on the amplitudes and cross-phase between density and poloidal electric field fluctuations (see Figure 6) [27]. Typically, the particle flux induced by AEs was found to vary widely from a negligibly low level up to being comparable to the flux induced by broadband turbulence.

4. L-H transition studies.

Tokamaks and stellarators develop edge plasma bifurcations with similar properties. In the TJ-II stellarator, spontaneous Low to High (L-H) transitions are achieved [28] under NBI

heating conditions when operating with lithium coated walls [14]. H-mode transitions reproduce common features found in other devices [3]: i.e. an increase in plasma density and plasma energy content, a reduction in H_α signal, the development of steep density gradients and a drastic reduction in the level of turbulence. For high power, high density plasmas the confinement improvement associated to the L-H transition reaches up to 40% [16].

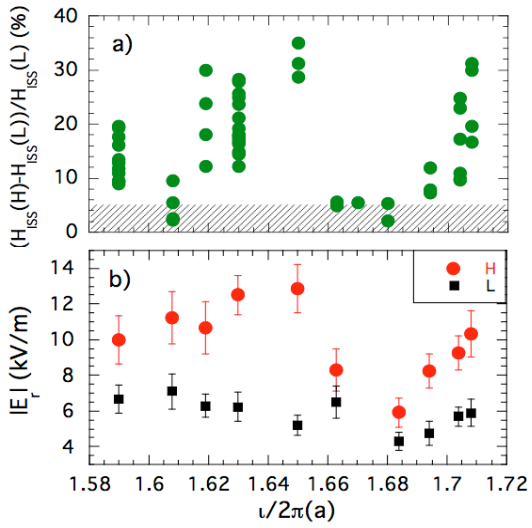

Figure 7: *(a) Increase of the H factor over the L-mode value and (b) absolute value of the radial electric field measured right before the L-H transition (squares) and during the H-mode (circles) at r = 0.75-0.8 as a function of edge iota.*

A fine rotational transform scan performed close to the L-H transition power threshold shows that both, the confinement enhancement factor and the shear of the radial electric field, increase at the L-H transition by an amount that depends on the magnetic configuration [16]. Both magnitudes show similar ι-dependence (see Figure 7): higher values are obtained in certain windows of the edge rotational transform, i.e., in configurations with a low order rational (5/3 or 8/5) close to the plasma edge. The results indicate a preferential radial position for the rational to ease the transition. In these configurations, pronounced oscillations in radial electric field are detected at the transition that are absent in configurations without low order rational surfaces.

The radial electric field, as measured by Doppler reflectometry [2], is of the order of 5 kV/m in the L-mode and increases up to 15 kV/m in the H-mode with a concomitant development of a strong *ExB* sheared flow in the proximity of ρ ≈ 0.85. At this radial position the density fluctuation level is reduced by a factor of 10; it should be noted that this reduction is strongly localized at the position of the maximum in the radial electric field shear (see figure 8).

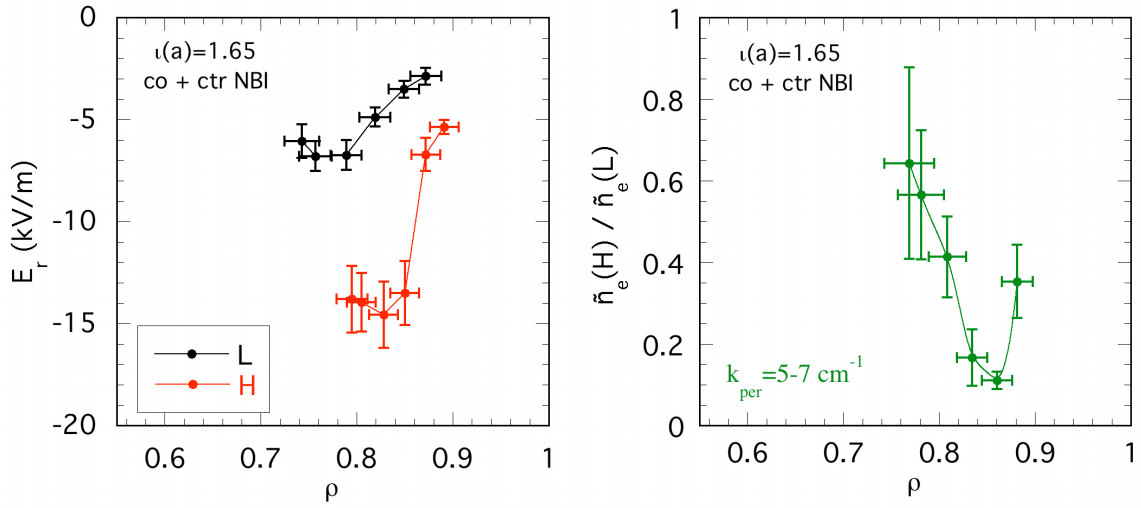

Figure 8: *Doppler reflectometry measurement showing: (left) Radial electric field profiles measured during the L and H-modes and (right) density fluctuation reduction at the perpendicular wave-number range 5-7 cm^{-1}.*

Besides the observation of a significant sheared radial electric field during the spontaneous L-H transition, an important result is the observation of remarkable fluctuating radial electric fields (in the frequency range of 1- 10 kHz) during the development of edge bifurcations [28]. In particular, high temporal and spatial resolution measurements using Doppler reflectometry indicate that the turbulence reduction precedes the increase in the mean sheared flow, but is simultaneous with the increase in the low frequency oscillating sheared flow (see Figure 9). Close to the transition threshold, a coupling between sheared flows and turbulence level is measured which reveals a characteristic predator-prey behaviour consistent with L-H transition models based on turbulence driven flows [29].

Radial profile of long-range correlation in density and potential fluctuations has been investigated in the SOL and edge plasma region of the TJ-II stellarator using two Langmuir probe arrays, named Probe 1 and Probe 2, installed on fast reciprocating drives located at two different toroidal locations. In these experiments Probe 1 is moved radially while Probe 2 is kept fixed at r/a ≈ 0.9. The toroidal correlation of density fluctuations is very low. On the contrary, the correlation between floating potential signals is significant (up to 0.8); the maximum of the correlation of the floating potential is observed when the probes are approximately at the same radial location in the plasma edge. These results are plotted in Figure 10 (left). The radial decay length of long-range correlations towards the Scrape-Off-Layer region is of the order of 1 cm. It should be noted that long-range correlations due to the emergence of Geodesic Acoustic Modes (GAMs) has been observed both in density and potential fluctuations in different fusion devices, whereas zonal flows do not show significant density fluctuation correlations. Recent experimental findings show that radial transport is reduced in the region dominated by the presence of long-range toroidally correlated structures (zonal flows) [30].

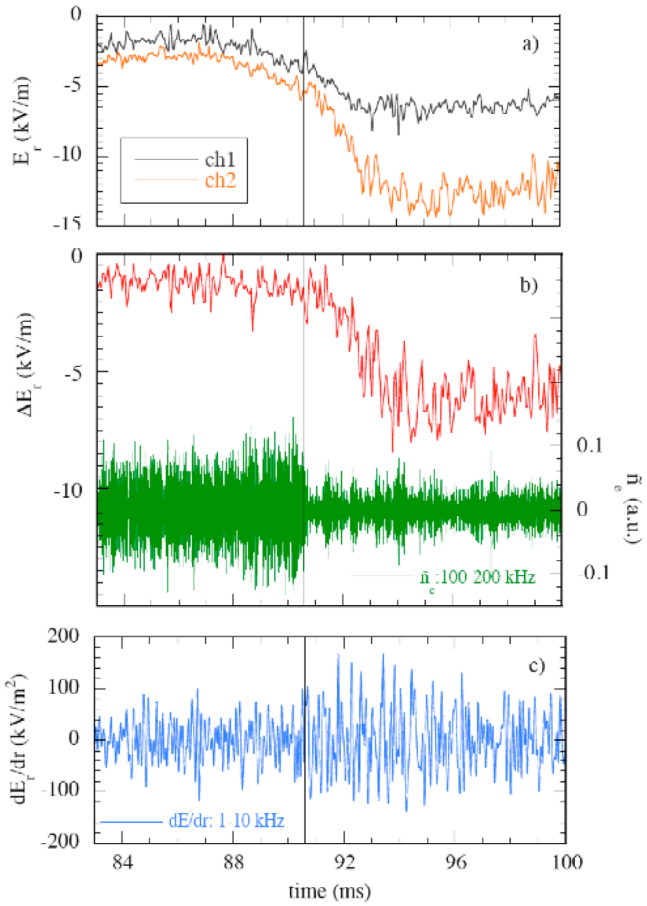

Figure 9: *Time evolution of E_r at two adjacent radial positions (a), their difference and the high frequency density fluctuations (b) and the low frequency fluctuations in E_r shear (c); plasma heated by both NBIs in the configuration i(a)=1.65. The vertical line indicates the L-H transition time.*

The correlation length of the plasma potential becomes of the order of the machine size during the L-H transition, quite unlike the density fluctuations [31]. These results show that the increase in the degree of long-range correlation is strongly coupled to the presence of mean radial electric fields. Figure 10 (right) plots the correlation as a function of density in order to see

the increase of coherency for the low density and the L-H transitions observed in TJ-II. The observed interplay between mean ExB shear flows and the development of low frequency (zonal flow like) structures could be explained considering the role of electric fields as a turbulence symmetry-breaking mechanism i.e. amplifying Reynolds stress driven flows [32]. Furthermore, the degree of long-range toroidal correlations is modulated during fine dynamical scans in the magnetic configuration in the proximity of low order rational surfaces, consistent with the theory of zonal flows linked to the magnetic topology in low magnetic shear configurations [31].

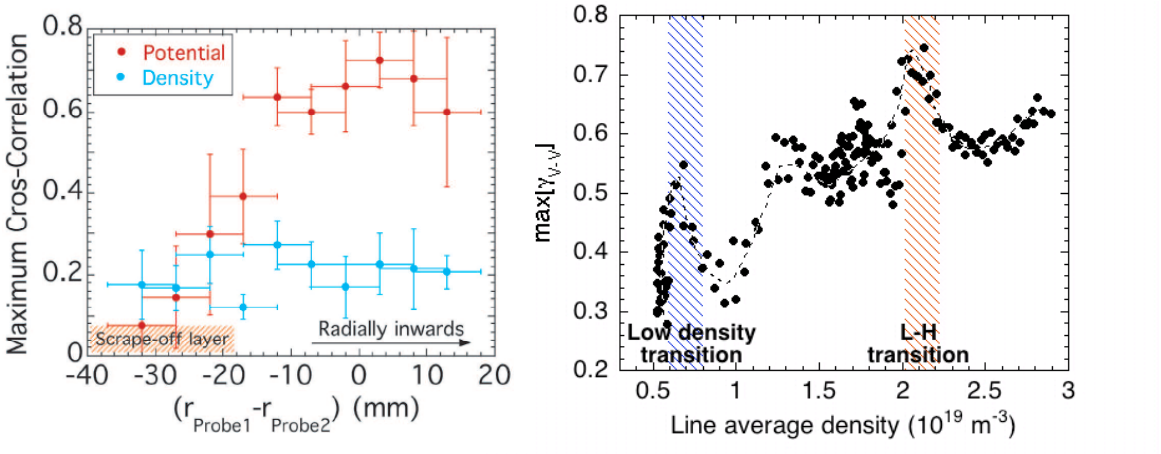

Figure 10. *Maximum value of the long-range cross-correlation function for potential fluctuations, as a function of: (left) radial position and (right) plasma density.*

5. Conclusions

Recent TJ-II experimental results are presented in this paper. We have continued with the characterization of plasmas under Li-coating walls, which has allowed to enlarge the operational density range and to reach H-mode customarily. The energy confinement time increases substantially for high density plasmas even in L mode. The properties of Li on the wall have been studied including the Li sputtering under H and He plasmas. The sputtering and desorption characteristics of H and He plasmas on a Li surface have been investigated in TJ-II, showing in particular that the threshold for Li sputtering and for H desorption are very similar in He plasmas, which suggests that both species could obey to the same release mechanism. However, a higher mass than that of LiH would be still required to explain the experimental energy values. Laboratory experiments are in progress to check the influence of the underlying B layer on these findings. The properties of fast ion confinement are also described, showing the appearance of Alfven modes, as well as the effects of impurities on radiation profiles, showing two types of emissivity profiles the “bell” and the “dome” shape, being the latter more robust under radiative collapse. The transition from one type of profile to another has been provoked dynamically in a single discharge by impurity puffing.

The L-H transitions have shown the development of long range correlations of the turbulent floating potential in the plasma edge coupled to the presence of mean and fluctuating radial electric fields. These findings provide a new guideline for understanding the trigger mechanisms of the L-H transition, pointing out the importance of low frequency fluctuating sheared ExB flows. These long-range toroidal correlations are modulated during fine dynamical scans in the magnetic configuration in the proximity of low order rational

surfaces, which is consistent with the theory of zonal flows linked to the magnetic topology. The low order rational surfaces located in the edge also provoke a better quality H-mode.

References

[1] GÓMEZ, A., CASTEJÓN, F., BUSTOS, A., and M.A. IAEA THC/P5-01.
[2] HAPPEL, T. et al., "Doppler reflectometer system in the stellarator TJ-II". Review of Scientific Istruments 80 (2009) 073502
[3] MELNIKOV, A.V., et al., "Internal measurements of Alfvén eigenmodes with heavy ion beam probing in toroidal plasmas" Nuclear Fusion 50 (2010) 084023
[4] PEDROSA, M.A. et al., "Evidence of long distance correlation of fluctuations during edge transitions to improved confinement regimes in the TJ-II stellarator" Review Letters 100 (2008) 215003
[5] GUZMÁN, F. et al., "On the determination of edge Ti profiles by a supersonic He beam in TJ-II". Journal of Nuclear Materials 390 (2009) 1127.
[6] JIMÉNEZ-REY, D., et al., Review of Scientific Instruments 79 (2008) 93511
[7] ARÉVALO, J., MCCARTHY, K.J., CARMONA, J. M., FONTDECABA, J. M., "Impurity Temperature Correction Factors for the Transmission Grating Spectrometer in the TJ-II stellarator". Review of Scientific Instruments (2010). In press.
[8] ESTEBAN, L., SÁNCHEZ, M., SÁNCHEZ, J., KORNEJEW, P., HIRSCH, M., LÓPEZ, J. A., FERNÁNDEZ, A., NIETO-TALADRIZ, O., "Continuous phase measurement in the W7-X IR interferometer by means of an FPGA and high speed ADCs", Fusion Science and Technology. In press.
[9] BAIÃO, D., et al., "Implementation of multi-filter based twin-prototypes for core electron temperature measurements in the TJ-II stellarator". Review of Scientific Instruments (2010). In press.
[10] VEGA, J., MURARI, A., RATTÁ, G.A., GONZÁLEZ, S., DORMIDO-CANTO, S., and JET-EFDA CONTRIBUTORS. "Progress on statistical learning systems as data mining tools for the creation of automatic databases in Fusion environments". Fusion Engineering and Design. 85 (2010) 399-402
[11] CASTEJÓN, F., CAPPA, Á., TERESHCHENKO, M., and FERNÁNDEZ, Á., "Computation of EBW heating in the TJ-II Stellarator" Nuclear Fusion 48 (2008) 075011.
[12] GARCÍA-REGAÑA, J. M., CASTEJÓN, F., CAPPA, A., TERESHCHENKO, M., and MARUSHCHENKO, N. B., "Comparison of different models for EBCD calculation in the TJ-II Stellarator" Plasma Physics and Controlled Fusion 52 (2010) 065007
[13] VELASCO, J.L., et al., IAEA THW/P7-16
[14] TABARÉS, F.L., et al., Plasma Physics and Controlled Fusion 50 (2008) 124051
[15] ASCASÍBAR, E., et al., "Global energy confinement studies in TJ-II NBI plasmas". Contributions to Plasma Physics. 50 (2010) 594
[16] ESTRADA, T., et al., "L-H transition experiments in the TJ-II stellarator". Contributions to Plasma Physics 50 (2010) 501
[17] TAFALLA, D., et al., Journal of Nuclear Materials, 2010. In press.
[18] OCHANDO, M.A., et al., "Nitrogen-injection effects on NBI heated TJ-II plasma profiles under Li wall conditions: impurity screening and role of rational surfaces". P1.1075, 37th EPS Conf. on Plasma Phys., Dublin, Ireland 2010.
[19] ZURRO, B., et al. IAEA EXC/P8-23.
[20] LÓPEZ-BRUNA, D., et al., "Magnetic resonantes in ECR-heated plasmas of the TJ-II Heliac" Contributions to Plasma Physics 50 (2010) 600

[21] BONDARENKO, O., et al., "Influence of low-order rational surfaces on the radial electric field of TJ-II ECH plasmas", Contribution to Plasma Physics. 50 (2010) 605
[22] REYNOLDS, J.M., LÓPEZ-BRUNA, D., Physics of Plasmas 17 (2010) 072504
[23] NARUSHIMA, Y., et al., IAEA EXS/P8-02
[24] MCCARTHY, K.J., TRIBALDOS, V., ARÉVALO, J., and LINIERS, M. "The detection of fast oxygen ions in neutral beam heated plasmas of the TJ-II stellarator using spectroscopy methods," J. Physics B: Atomic, Molecular and Optical Physics 43 (2010) 144020.
[25] JIMÉNEZ, R., et al., "Alfvén eigenmodes measured in the TJ-II stellarator". Nuclear Fusion (2010). Submitted.
[26] BUSTOS, A., et al. IAEA THW/P7-03
[27] MELNIKOV, A., et al. IAEA EXW/P7-17
[28] ESTRADA, T., et al., "Sheared flows and transition to improved confinement regime in the TJ-II stellarator". Plasma Physics and Controlled Fusion 124015 (2009) 51
[29] ESTRADA, T., et al., IAEA EXC/P3-01
[30] PEDROSA, M. A., et al., IAEA EXC/P3-04
[31] HIDALGO, C., et al., "Multi-scale physics mechanisms and spontaneous edge transport bifurcations in fusion plasmas". Europhysics Letters 87 (2009) 55002
[32] ALONSO, J.A., HIDALGO, C., PEDROSA, M.A., and PABLOS, JL, "On the link between parallel flows, turbulence and electric fields in the edge of the TJ-II stellarator". Europhysics Letters 87 (2009) 55002